Resonant Raman spectroscopy of deformed single-walled carbon nanotubes under both torsional and tensile strain

Xiaowei Li,[1] Yonglei Jia,[1] Jinming Dong,[1,*] and Yoshiyuki Kawazoe[2]

[1]*Group of Computational Condensed Matter Physics, National Laboratory of Solid State Microstructures and Department of Physics, Nanjing University, Nanjing 210093, People's Republic of China*

[2]*Institute for Materials Research, Tohoku University, Sendai 980-8577, Japan*

The first-order resonant Raman spectra of the deformed single-walled carbon nanotubes (SWCNTs), suffered from both tensile and torsional strains, have been studied within the nonorthogonal tight-binding model. It is found that: (1) two kinds of the strains almost do not change the frequencies of the low-energy Raman modes. In contrast, the tensile strain downshifts all the G-band Raman modes, but the torsional strain-induced G-band shifts depend on the tube's chirality and the mode symmetry. (2) The changes in resonant Raman intensity depend on the strain type, mode symmetry, and the selected electronic transition energy. For example, the torsional strain increases (decreases) the TO (LO) mode intensity, and the tensile strain has little effect on that of the TO mode but increases or decreases the LO mode intensity, depending on the electronic transition energy. (3) More importantly, when both the tensile and torsional strains are simultaneously applied to the SWCNTs, there would be an interference effect between two kinds of strains on the strain-induced frequency shifts and intensity changes, which are not equal to a simple sum over those induced separately by tensile and torsional strains, and the interference effect is found to depend on the tube chirality and mode symmetry, which has already been partially supported by the experimental observations.

I. INTRODUCTION

Carbon nanotube (CNT) stimulated a great interest in the nanoscience and nanotechnology since it was discovered in 1991 by Iijima[1] because of its exceptional mechanical, electronic, and optical properties.[2] The CNT can be seen as a seamless cylinder with a nanometer-scale diameter, obtained by wrapping a graphene sheet.

At the present time, much attention has been paid to the CNT's resonant Raman spectroscopy because of its nondestructive advantage to study the CNT's physical properties. When the laser energy of either the incident or the scattered light matches the van Hove singularities (vHSs) in the CNT's joint density of states (JDOS), satisfying the resonance condition, the Raman intensity becomes extremely strong for any CNT.[3] As for the first-order Stokes process, there would be two peaks near the E_{ii} and $E_{ii}+\hbar\omega_q$, where E_{ii} is the electronic transition energy between the electronic valence and conduction bands[4] and ω_q is the phonon frequency. So the Raman spectroscopy has been considered a powerful tool to detect the CNT's phonon modes,[5,6] among which the radial breathing mode (RBM) and the tangential G-band modes ($2A_1$, $2E_1$, and $2E_2$) are two particularly important ones for the single-walled carbon nanotubes (SWCNTs).[3,7]

The physical properties of the deformed SWCNTs have been studied by a lot of theoretical and experimental works.[8–32] There are many experiments on the frequency shifts of the RBM and G-band modes of individual SWCNT under a strain, induced by the AFM tip or an applied pressure.[8–14] For example, tensile strain is found to lower the frequencies of G-band modes but keep that of the RBM mode unchanged, which could change the intensity of resonant Raman spectra.[10–12] On the other hand, the theoretical calculations have shown that tensile or torsional strain can

change greatly the electronic structures of the deformed SWCNTs,[15–19] which have been confirmed by some experiments.[20–26]

The Raman spectra of both the RBM and high-energy modes for the strained[27] or perfect[28–32] SWCNTs have been calculated by the *ab initio* and tight-binding (TB) methods. Wu *et al.*[27] made the *ab initio* calculations of the nonresonant Raman spectra of the deformed SWCNTs under only tensile or torsional strains based upon the empirical bond polarizability model.

However, up to now, there are much less experimental works on the deformed SWCNTs, suffering simultaneously from both tensile and torsional strains. Only recently, could Duan *et al.*[8] study the resonant Raman spectra of individual deformed SWCNTs under both tensile and torsional strains, finding the different effects of torsional strain on the Raman spectra of deformed SWCNTs from those of uniaxial strain, and the significant difference of different vibration modes in response to both the strains. Nevertheless, there still has no corresponding theoretical works on the resonant Raman spectra of deformed SWCNTs under both tensile and torsional strains up to now.

Therefore, in this paper, we have calculated the resonant Raman spectra of deformed SWCNTs when both tensile and torsional strains are simultaneously applied on them using the nonorthogonal TB model. It is found that the frequency shifts of low- and high-energy Raman modes are different for the two strains, which also depend on the tube's chirality and mode symmetry, and the resonant Raman intensity will change with applied strains, depending on the mode symmetry, electronic transition energy and deformation type. More importantly, we have found existence of an interference effect on the strain-induced frequency shifts and intensity changes due to both the strains, which are not equal to a
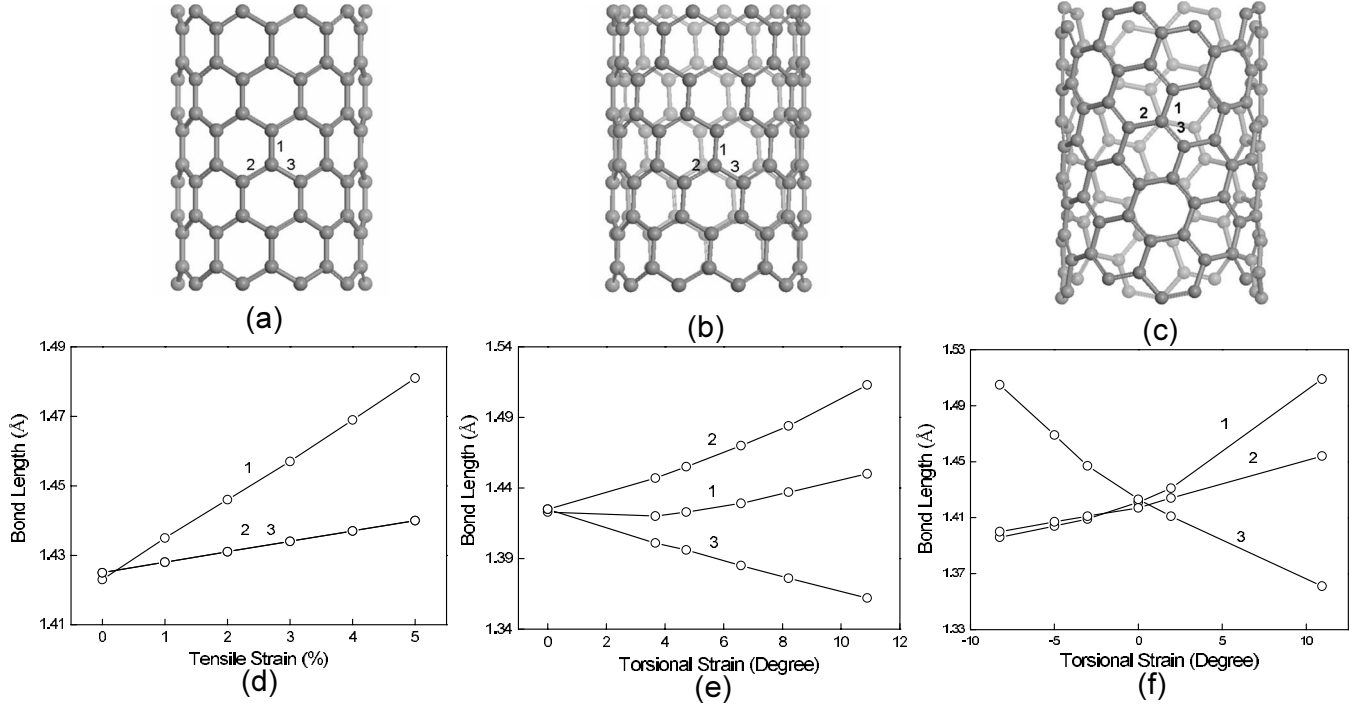
FIG. 1. The geometrical structures of (a) undeformed (10,0) SWCNT, and (b) deformed one under a torsional strain of 6.59° and (c) undeformed (8,4) SWCNT. (d) and (e) denote length changes of the three nearest C-C bonds of (10,0) tube, signed as 1, 2, and 3 in (a) and (b), under pure tensile and torsional strains, respectively. (f) denotes length changes of the three nearest C-C bonds of (8,4) tube under the positive and negative torsional strains.

simple sum over those induced separately by tensile and torsional strains, and the interference effect depends on the tube's chirality and mode symmetry.

This paper is organized as follows. In Sec. II, the theoretical model and calculation details are presented. In Sec. III, the changes in resonant Raman spectra induced by tensile and torsional strains are discussed.

II. THEORETICAL MODEL AND CALCULATION DETAILS

The first-order resonant Raman intensity per unit length in the Stokes process is given as follows:[3,7]

$$I = C(n_{ph} + 1)T\left(\frac{E_s}{E_a}\right)^2$$
$$\times \left| \frac{1}{T}\sum_{c\nu} \frac{M_{op}^* M_{e-ph} M_{op}}{[E_L - E_{c\nu} - i\gamma][E_L - E_{c\nu} - E_{ph} - i\gamma]} \right|^2. \quad (1)$$

Here, $E_{ph} = \hbar\omega$ is the phonon energy and $n_{ph} = 1/(e^{-\beta E_{ph}} - 1)$ is the phonon distribution function. E_L is the incident laser energy. C is a tube-independent constant and T is the supercell's length. E_a and E_s are the absorption and emission photon energies, respectively. $E_{c\nu} = E_c - E_\nu$ denotes the electronic transition energy and γ is the broadening factor. M_{op} and M_{e-ph} are the electron-photon and electron-phonon interaction matrix elements, respectively, for which the M_{op} is calculated following Refs. 33 and 34, and the M_{e-ph} is given by[32]

$$M_{e-ph} = \sqrt{\frac{\hbar}{2M_C N\omega}}[M(c,k) - M(\nu,k)]. \quad (2)$$

Here,

$$M(n,k) = \sum_{jj'} c_{nkj}^*(\delta H_{nkjj'} - E_{nk}\delta S_{nkjj'})c_{nkj'}, \quad (3)$$

where, $\delta H_{nkjj'}$ and $\delta S_{nkjj'}$ are the phonon's perturbations to the Hamiltonian matrix elements $H_{nkjj'}$ and the overlap ones $S_{nkjj'}$, respectively, due to the phonons. The M_C and N refer to the mass and the number of carbon atoms.

We have calculated the first-order Resonant Raman spectra of the deformed zigzag (10,0), (9,0), and (8,0) SWCNTs, the armchair (6,6) and (5,5) ones, and the chiral (8,4) tubes within the nonorthogonal TB model, in which the parameters are taken from the density-functional calculations.[35] In our calculations, the tensile strain is defined as $\varepsilon = T/T_0 - 1$,[27] where T and T_0 are the unit cell lengths of the deformed and undeformed tubes, respectively, and the definition of the torsional angle is similar to that in Refs. 18 and 19. Taking as an example, the geometrical structures of the undeformed and torsion-strained (10, 0) SWCNT, and also the undeformed (8,4) one are shown in Figs. 1(a)–1(c), respectively.

III. RESULTS AND DISCUSSIONS

Let us firstly study in Sec. III A the deformation-induced frequency shifts of the Raman modes, and then do in Sec. III B the resonant Raman intensity changes.
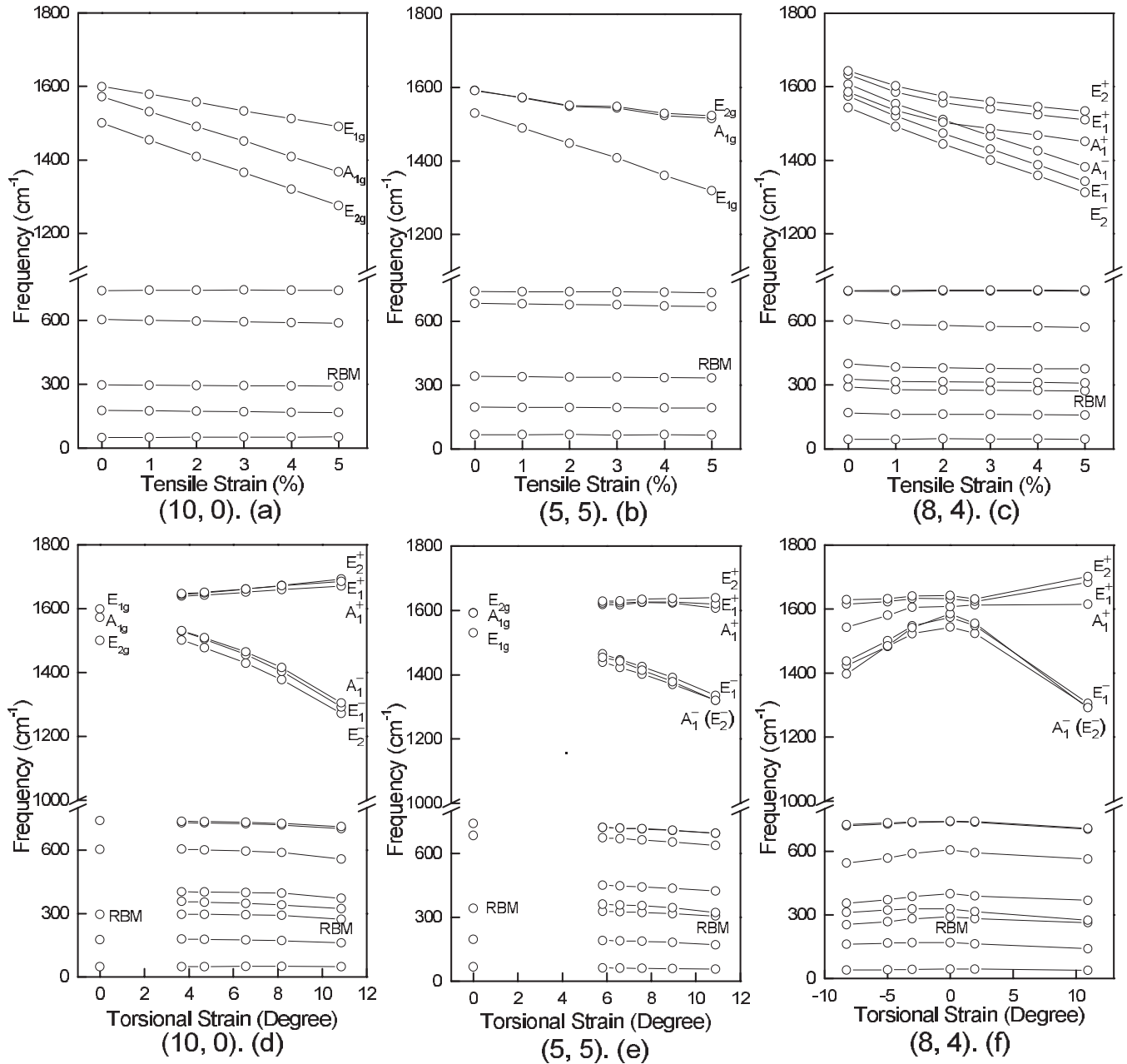
FIG. 2. Raman-active mode's frequencies of the deformed (10,0), (5,5), and (8,4) SWCNTs vary with pure tensile strains in (a)–(c) and with pure torsional strains in (d)–(f), respectively.

A. Frequency shifts of the Raman-active vibrational modes

The calculated frequency shifts of the Raman-active modes for three different (10,0), (5,5), and (8,4) SWCNTs under only tensile strains are given in Figs. 2(a)–2(c), respectively, from which it can be seen that the frequencies of low-energy Raman modes, including the RBM, almost do not change by tensile strains, in contrast to the remarkable frequency shifts of high-energy Raman modes, which is well consistent with the experimental observations.[8,12] It is found that tensile strains downshift the G-band frequencies of all the calculated SWCNTs, which has only a weak relation with the tube's chirality and Raman mode symmetry.

As shown in Fig. 2, there are three high-energy Raman modes (A_{1g}, E_{1g}, and E_{2g}) for achiral (10,0) and (5,5) tubes,

but six ones (A_1^+, E_1^+, E_2^+, A_1^-, E_1^-, and E_2^-) for chiral (8,4) tube. When tensile strains are applied, these Raman modes are found to still exist since the original tube symmetry is not broken by tensile strain. However, with increasing tensile strain, the frequencies of some G-band modes are found to decrease more quickly than others, presenting different frequency variation slopes for different Raman modes. For example, it is seen from Fig. 2(a) that when tensile strain increases, the frequencies of A_{1g} and E_{2g} modes of (10,0) tube decease more quickly than that of its E_{1g} mode. But the situation is reversed for armchair (5,5) tube, as shown in Fig. 2(b), for which the frequency of its E_{1g} mode deceases more quickly than those of its A_{1g} and E_{2g} modes. As for chiral (8,4) tube, the situation becomes more complicate, in which

the frequencies of its E_2^- and E_1^- modes decrease more quickly than those of its other modes, and there is a cross point between its two A_1^+ and A_1^- modes, as shown in Fig. 2(c).

The above calculated results that the *G*-bands downshift with increasing alone tensile strain, while the RBM remains unchanged, are well consistent with the experimental observations in Ref. 12, but only accord partially with those observed in Ref. 8 because in the latter experiment, the highest frequency *G*-band mode (ω_{G1}) of the semiconducting SWCNTs was insensitive to tensile strain although other five *G*-band modes were observed to downshift with increasing tensile strain. We think this inconsistence between our calculation results and the experimental ones in Ref. 8 probably is caused by the following fact that the experiment was made under both tensile and torsional strains, making very difficult to accurately separate the respective contributions from both the strains. So, perhaps more fine experimental studies and also numerical calculations are needed to solve this problem.

The downshift of the *G* band with increasing tensile strain can be understood on the basis of the C-C bond elongations. Let us take (10,0) tube as an example. For the undeformed (10,0) tube, the lengths of its three nearest C-C bonds, 1, 2, and 3 [shown in Fig. 1(a)] are found to be 1.423, 1.425, and 1.425 Å, respectively, which would be elongated by tensile strains, showing a linear increase with increasing tensile strain, as clearly seen from Fig. 1(d). But the length of bond 1, which is parallel to tube axis, increases more quickly than those of other two bonds 2 and 3, almost along the circumferential direction. It is known that in both the A_{1g} and E_{2g} modes, the atomic vibrations are along tube axis, making so their frequency shifts depend mainly on the bond 1. On the other hand, the E_{1g} mode corresponds to the vibrations along circumferential direction, and so its frequency shift should mainly depend on the bond 2 and 3. That is why with increasing tensile strains, the former two mode's frequencies decrease more quickly than the latter one.

Now, let us study the torsional strain effects on the SWCNT's Raman modes, which are found to be greatly different from those of the tensile one because the former breaks the original symmetry of achiral SWCNTs. So, torsional strain would increase the Raman mode number,[27] and induce the complex *G*-band frequency shifts, depending strongly on the tube's chirality and Raman mode symmetry. The calculated frequency shifts of the Raman modes for three (10,0), (5,5), and (8,4) tubes under pure torsional strains are given in Figs. 2(d)–2(f), respectively.

It is seen from Figs. 2(d) and 2(e) that the original three high-energy Raman modes of undeformed achiral (10,0) and (5,5) tubes split into the six (A_1^+, E_1^+, E_2^+, A_1^-, E_1^-, and E_2^-) under a torsional strain. Also, the frequencies of these six modes change differently with increasing torsional strain, following two different routes, among which the frequencies of minus (−) branch, i.e., the A_1^-, E_1^-, and E_2^- modes, downshift greatly with increasing torsional strain, but those of plus (+) branch, i.e., the A_1^+, E_1^+, and E_2^+ modes, change slowly, depending much on the tube's chirality. For example, the frequencies of A_1^+, E_1^+, and E_2^+ modes of zigzag (10,0) tube upshift slightly with increasing torsional strain. But, those of armchair (5,5) tube are nearly not changed by torsional

strain. The situation becomes different for chiral (8,4) tube, as shown in Fig. 2(f), for which there already exist six high-energy Raman modes at zero torsional strain, and their frequency shifts exhibit a different behavior from those of achiral (10,0) and (5,5) tubes. Firstly, its *G*-band frequency shifts are obviously unsymmetric to the positive and negative torsional strains, among which particularly obvious are its plus (+) modes (A_1^+, E_1^+, and E_2^+). For example, the frequencies of its E_1^+ and E_2^+ modes are almost not changed by a negative torsional strain, in contrast to their increase under a positive one, and its A_1^+ mode frequency is decreased by the negative torsional strain, but increased a little by the positive one. Secondly, the frequencies of its minus (−) modes decrease greatly with increasing torsional strain.

The reason behind them can also be found from different length changes of the three nearest C-C bonds, induced by torsional strains, which are described in Figs. 1(e) and 1(f) for (10,0) and (8,4) tubes, respectively. It can be seen from Fig. 1(e) that the bond 1 is slightly shortened by the smaller torsional strain (less than about 4°), which, however, will become longer with further increasing torsional strain. The lengths of other two bonds 2 and 3 will be changed oppositely, among which the length of bond 2 becomes longer (but that of bond 3 shorter) than the perfect ones under all the torsional strains. It is known that the atomic vibrations in the A_1^-, E_1^-, and E_2^- modes are mainly along bonds 1 and 2, making the G^- mode frequency of (10,0) tube to decrease with increasing torsional strain. On the other hand, the atomic vibrations in the A_1^+, E_1^+, and E_2^+ modes are mainly along the bond 3, making so their frequencies to increase gradually with increasing torsional strain. For (8,4) tube, its C-C bond changes are unsymmetrical under the positive and negative torsional strains, as described in Fig. 1(f), which so makes its *G*-band mode frequencies to be changed unsymmetrically under the positive and negative torsional strains.

On the other hand, as shown in Figs. 2(d)–2(f), the low-energy modes are less influenced by torsional strain, except that some new modes appear around 400 cm^{-1} for achiral tubes, which is consistent with the experimental observation.[8] Particularly, the RBM frequency is not changed either or decreases a little with increasing torsional strain for armchair (5,5) and chiral (8,4) tubes, contradicting the experimental results in Ref. 8, which found the RBM frequency increases a little with increasing torsional strain. This contradiction has not been understood, which needs more theoretical and experimental studies.

Our calculated results of the torsional strain effects are also partially consistent with the experimental observations in Refs. 8 and 24, e.g., under torsional strain, some *G*-band modes (G^+ modes) upshift and some (G^- modes) downshift, showing clearly that the torsional strain effect on the *G*-band modes indeed depends on the mode symmetries, and also the frequency downshift is always much larger than the frequency upshift for all the SWCNTs we have studied. Comparing with the experimental observations, we have found also inconsistencies between our calculated results and the experimental ones. For example, the experiment found that with increasing torsional strain, there is only one *G*-band mode (always the highest frequency one, claimed to be the E_2^+ mode), downshifting greatly (reaching to about
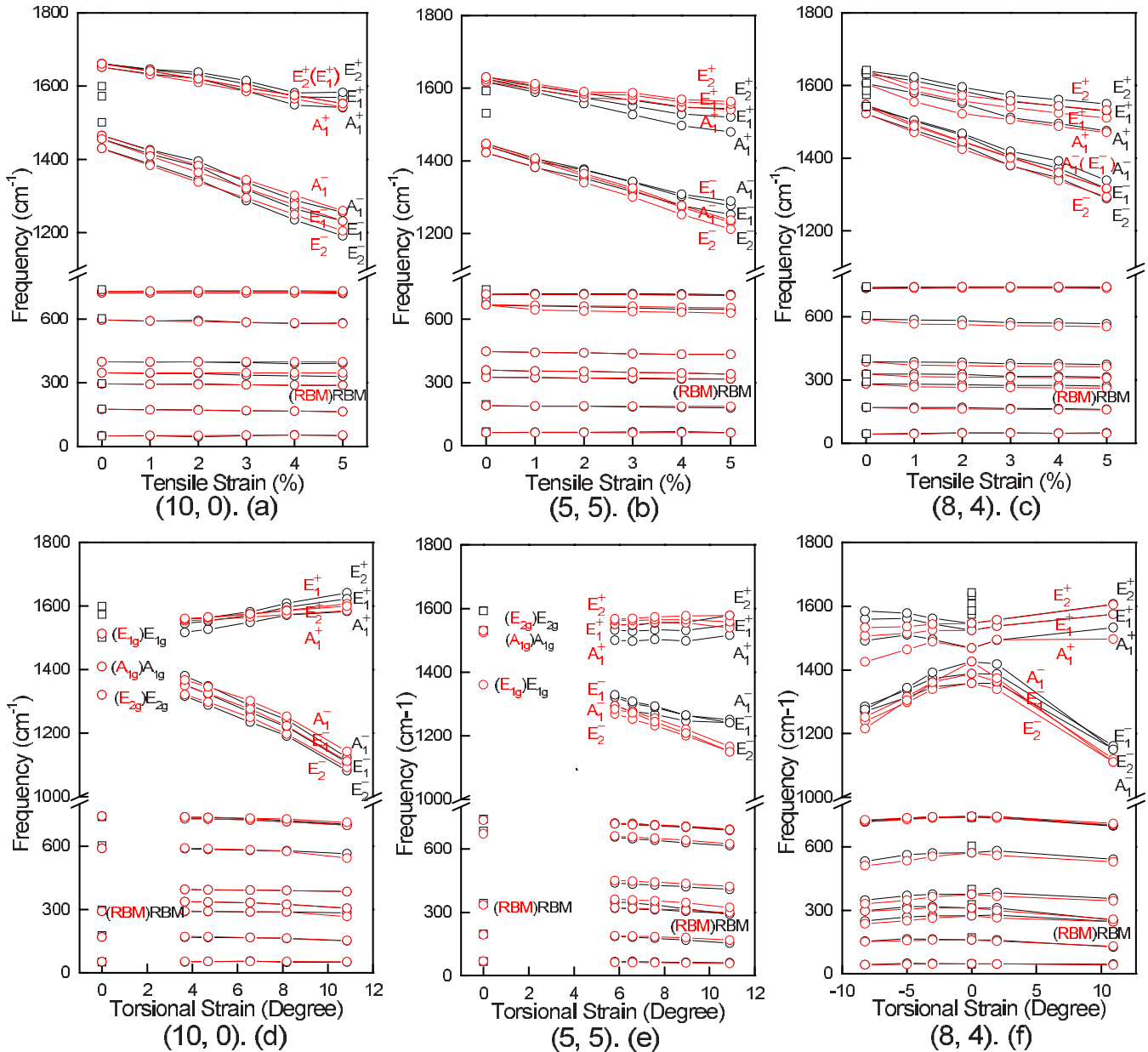
FIG. 3. (Color online) Raman-active mode's frequencies of the deformed (10,0), (5,5), and (8,4) SWCNTs vary with tensile strains at a fixed torsional strain of 6.6°, 6.6°, and −3.0°, respectively, in (a)–(c). (d)–(f) show the similar variations, but with torsional strains at a fixed tensile strain of 4%. Here, the light (red online) dot lines denote the simple summations of those shifts, induced by the separate tensile and torsional strains. The black squares denote the Raman-active mode's frequencies of the perfect tubes.

90 cm^{-1}), but all other G-band modes upshift a few cm^{-1}. In contrast, our calculations found that with increasing torsional strain, there are always three G^- modes, downshifting greatly [reaching to about 290 cm^{-1} at a torsional strain of 11° for the A_1^- mode of (8,4) tube], and other G^+ modes upshift a little [about 90 cm^{-1} at a torsional strain of 11° for the E_2^+ mode of (8,4) tube]. The above inconsistencies, most probably, come from the complicate conditions in the experiment, e.g., the varying strain intensity (both the tensile and torsional) along the tubes and substrate effects. So, more experimental and theoretical investigations are needed to identify these inconsistencies.

Now, it is very interesting to know what happens when the SWCNTs suffer simultaneously from both tensile and torsional strains. The calculated results are shown in Fig. 3. Let us firstly study the situations of varying tensile strain but at a fixed torsional one, which are shown in Figs. 3(a)–3(c), respectively, for deformed (10,0), (5,5), and (8,4) tubes. It is found from Figs. 3(a) and 3(b) that when a fixed torsional strain is applied to achiral (10,0) and (5,5) tubes, there appear six G-band modes (A_1^-, A_1^+, E_1^-, E_1^+, E_2^-, and E_2^+), and their frequencies make also a nearly linear decrease with increasing tensile strain, as like that happened without the torsional strain, shown in Figs. 2(a) and 2(b). However, their variation slopes with increasing tensile strain are different from those at zero torsional strain. For example, for (10,0) tube, suffering from pure 5% tensile strain, the frequencies of its A_{1g}, E_{1g}, and E_{2g} modes downshift by about 205.2,

108.7, and 224.7 cm^{-1}, respectively, as shown in Fig. 2(a). But by adding a torsional strain of 6.6°, its G-band modes firstly split into two groups: the minus (−) and plus (+) modes, and then downshift differently. The frequency splits between these two groups are different for the different modes, among which the split between the E_2^+ and E_2^- modes is the biggest, and that between the A_1^+ and A_1^- modes is the smallest, as seen obviously from Fig. 3(a). The frequencies of its A_1^-, E_1^-, and E_2^- modes are found to be downshifted by about 209.3, 224.6, 239.1 cm^{-1} at the largest tensile strain of 5%, respectively, in contrast to the downshifts of 101.4, 93.1, and 78.2 cm^{-1}, respectively, for its A_1^+, E_1^+, and E_2^+ modes. So, the frequency downshifts of its A_1^+ and E_2^+ modes are very different from those of its A_{1g} and E_{2g} modes at zero torsional strain, and similarly, the frequency downshift of its E_1^- mode is very different from that of its E_{1g} mode at zero torsional strain. Therefore, it can be concluded that when a varying tensile strain and a fixed torsional one are simultaneously applied on the achiral SWCNTs, the frequency downshifts of their high-energy G-band modes depend on the mode's types (+ or −) and symmetries (A_1, E_1, and E_2).

Another more interesting problem is whether or not above mentioned frequency shifts of the G-band modes, induced by the varying tensile strain at a fixed torsional one, equal to a simple summation over those induced by both of the separate tensile and torsional strains. In order to make it clear, we have also given the latter in Fig. 3, denoted by light (red online) dots. By comparing both of them, it is found that: (1) the differences between the former and the latter increase with increasing tensile strain. However, for the smaller tensile strains (<2%), the differences between both of them are small and could be neglected. (2) At the larger tensile strains (>2%), both of them are not equal any more. The latter G-band frequencies are larger or smaller than the formers, depending on the Raman mode's symmetry and the tube's chirality. For example, for (10,0) tube, its simple summation of the G^- band is larger than the combined result when tensile strain is above 2%; but that for the E_1^+ and E_2^+ band is lower than the combined results, which is particularly obvious for large tensile strain (e.g., larger than 4%), and for (5,5) tube, the simple summations for the G^+ modes are larger than the combined results; but that for the G^- band are smaller. For (8,4) tube, the simple summation for its E_1^+ and E_2^+ band is smaller than the combined result; but that for its G^- band is only a little bit smaller.

Next, let us discuss the opposite situations, i.e., varying torsional strain, but at a fixed tensile strain of 4% for (10,0), (5,5), and (8,4) tubes, which are shown in Figs. 3(d)–3(f), respectively. It can be seen that the frequency splits between the G^+ and G^- modes also become larger with increasing torsional strain, which is similar to those at zero tensile strain, i.e., under pure torsional strain, as shown in Figs. 2(d)–2(f). But they are also different from those under pure torsional strain because they are now superimposed on the additional frequency shifts, induced by the fixed tensile strain. For example, it is seen from Figs. 3(d)–3(f) that although the G^+ mode frequencies look to upshift with increasing torsional strain, they, in fact, make an overall downshift, if compared to their original frequencies (i.e., the values of

perfect tubes) since there is now a coexistence of the tensile strain of 4%. This result is well consistent with the experimental observations when there exist simultaneously the tensile and torsional strains.[8]

However, it is noted again that the frequency shifts due to varying torsional strain at a fixed tensile strain (referred as the combined results in the following) are not equal either to the simple summations over those induced by the separate tensile and torsional strain, as shown in Figs. 3(d)–3(f). For example, for (10,0) tube [Fig. 3(d)], the summed frequency for its G^+ band is larger or smaller than the combined one, depending on the torsional strain. At the smaller torsional strain (less than about 6.6°) the simple summation is larger than the combined one, but becomes smaller when torsional strain is larger than about 6.6°, and the simple summation for its G^- band is only a little bit larger than the combined one besides its A_1^- mode at the smaller torsional angle. But the situation becomes different for (5,5) tube [Fig. 3(e)], whose G-band mode is changed greatly by the addition of the fixed tensile strain, making the summed frequencies for the G^+ (G^-) modes are obviously larger (smaller) than the corresponding combined ones, especially at torsional strain smaller (larger) than 8.9°. Finally, for chiral (8,4) tube [Fig. 3(f)], the summed frequencies for all the G-band modes are smaller than the combined ones, especially at the negative torsional strains, except its E_2^+ and E_1^+ modes at the positive ones, for which the simple summation is equal to the combined result.

Thus, we can say that the frequency shifts of high-energy Raman modes, induced by both tensile and torsional strains, cannot be regarded as a simple sum over two separate contributions from only the tensile or torsional strain, which is particular obvious for the armchair tubes. It means an existence of an *interference* (or *cooperative*) effect between two different strains (the tensile and torsional ones) on the frequency shifts. On the other hand, however, the simple summation could be considered to be roughly equal to the combined result for chiral tubes, especially at the positive torsional strains, which means for chiral tubes, the so-called interference effect is weak. All these facts are obviously interesting and important, which could be demonstrated by future experiments.

We should emphasize that the above interference phenomenon between the tensile and torsional strains has already been partially observed in the experiment of Duan *et al.*,[8] which claimed that their ω_{G1} is always largely downshifted by torsional strain (the downshift can be as large as 90 cm^{-1}), demonstrating it is sensitive to torsional strain, but it is insensitive to uniaxial strain in their region II with a coexistence of the torsional and tensile strains. Their observation is in fact caused by the superposed tensile strain, which could be compared with our calculation results, shown in Figs. 3(d)–3(f). We can see from Fig. 3(f) that at a fixed tensile strain the combined result for the E_2^- mode, having a large downshift with increasing torsional strain, is larger than the simple summation. The same situation appears for the G^- band of (5,5) tube, as seen from Fig. 3(e). That means the E_2^- mode of chiral (8,4) tube and the G^- band of (5,5) tube become less sensitive to the tensile strain due to coexistence of both torsional and tensile strains (i.e., due to the interfer-
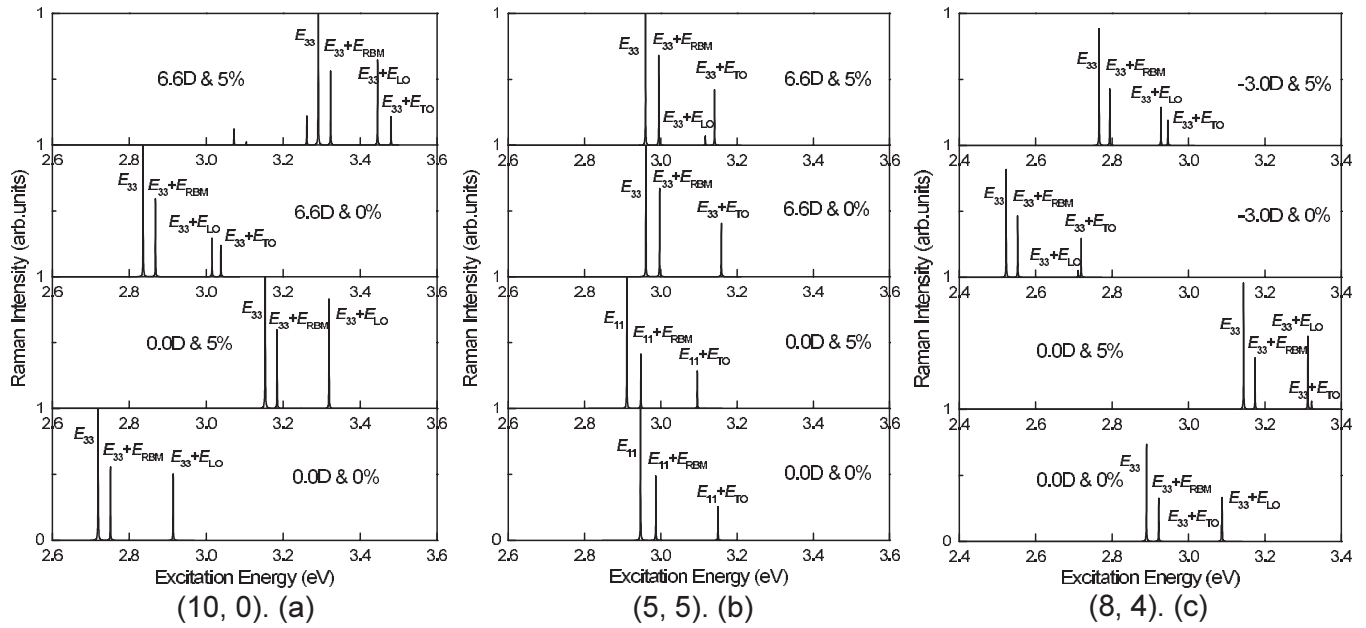
FIG. 4. The first-order resonant Raman spectra at the higher excitation energy for different SWCNTs under both tensile and torsional strains: (a) (10,0), (b) (5,5), and (c) (8,4) tubes, where those of the perfect tubes are also included for comparisons. The subfigures from the bottom to top of each figure denote, respectively, the results of the perfect tubes, the deformed ones under pure tensile strain, pure torsional strain, and both of them. The electronic transition energies E_{ii} ($i=1$ or 3) lie at about 3.0 eV. Here, the applied tensile strains are fixed at 5%, and the torsional ones are taken to be 6.6°, 6.6°, and −3.0°, respectively, for the (10,0), (5,5), and (8,4) tubes. In all the figures, the lower-energy mode is the RBM, and the higher-energy one is the G-band mode.

ence effect). But, as we can see from Fig. 3(d) that the situation becomes different for the zigzag tubes. Its E_2^- mode becomes *more* sensitive to the tensile strain due to the interference effect, because the combined result of its E_2^- mode becomes smaller than the simple summation, which is in good contrast against the (5,5) and (8,4) tubes. Therefore, the interference probably depends on the tube's chirality and mode symmetry, and especially plays a more important role in the armchair SWNTs, which also needs further experimental demonstration in future.

On the other hand, by comparing Fig. 3(f) with Fig. 2(f) at zero tensile strain, we have found that for the E_2^- mode of (8,4) tube, the superposed tensile strain makes its frequency-downshift rate with increasing torsional strain (22.9 cm^{-1}/deg, i.e., the shift amount/per tortional degree) to be smaller than that without tensile strain (25.4 cm^{-1}/deg). That means we can also say that the coexistence of two strains (or equivalently, the interference effect) makes the E_2^- mode of (8,4) tube to be *less sensitive* to the torsional strain. We hope this interesting phenomenon will be demonstrated in future fine experiments.

B. Changes in the first-order resonant Raman spectroscopy

In general, the resonant Raman intensity is closely related to the energy bands, electron-phonon interaction, and electron-photon interaction. Here, we have calculated the first-order resonant intensity of the Raman-active modes, taking the light polarization to be parallel to tube axis.

The calculated first-order resonant Raman spectra for three (10,0), (5,5), and (8,4) tubes are given in Fig. 4, in

which tensile strain is fixed at 5%, but torsional strains are taken to be 6.6°, 6.6°, and −3.0°, respectively, for (10,0), (5,5), and (8,4) tubes, and the resonance energy is taken to be the higher one of about 3.0 eV. For comparison, the first-order resonant Raman spectra of the corresponding three perfect tubes are also calculated and given in Fig. 4.

Let us firstly discuss zigzag (10,0) tube. It can be seen clearly from Fig. 4(a) that its Raman-active G-band LO mode intensity is increased by alone tensile strain by about 60% but decreased by alone torsional strain by about 50%, and its G-band TO mode intensity is no longer zero due to torsional strain. At the same time, its RBM mode intensity almost does not change due to torsional or tensile deformation. When both tensile and torsional strains are simultaneously applied, it is found that its LO mode intensity is increased by about two times, compared with that under pure torsional strain but decreased a little bit, compared with that under pure tensile strain. On the other hand, its TO mode intensity is nearly not changed, compared with that under pure torsional strain. So, it seems that the resonant Raman intensity of (10,0) tube under both tensile and torsional strains could be roughly considered as the simple summation over those contributions from the separate tensile and torsional strains.

For armchair (5,5) tube, it can be seen from Fig. 4(b) that tensile strain has little effect on the Raman intensity of its both RBM and TO modes, but torsional strain increases the Raman intensity of its RBM and TO modes by about 50% and 30%, respectively. However, we should mention that torsional strain makes the armchair (5,5) tube to become a semiconducting, and at a torsional strain of 6.6°, its resonant state at about 3.0 eV is also changed from the original E_{11} to
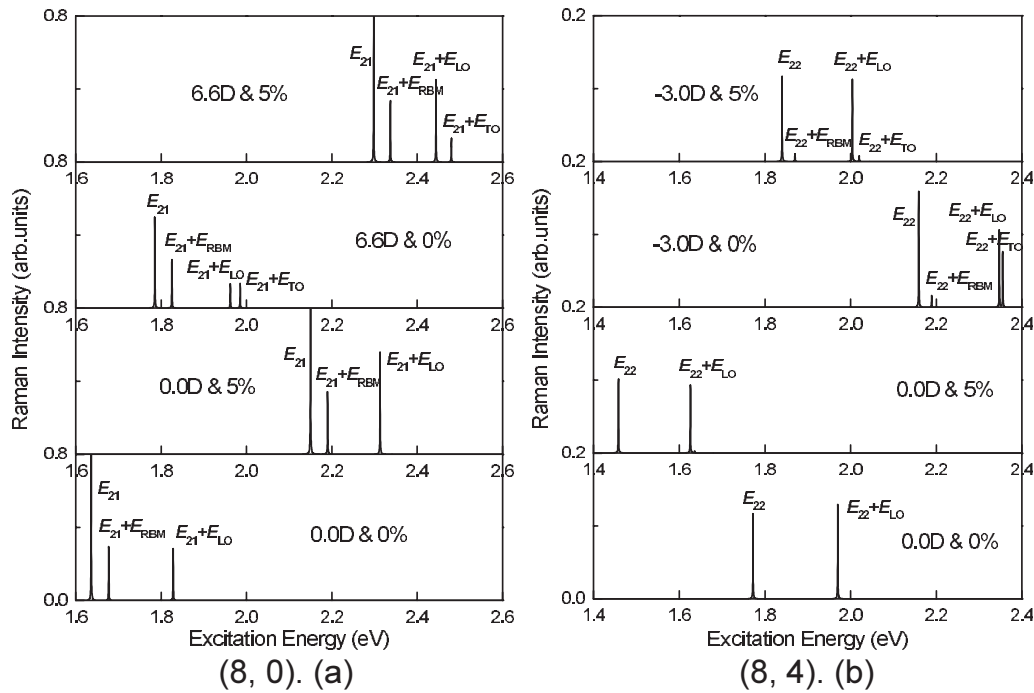
FIG. 5. The first-order resonant Raman spectra at the lower excitation energy for two semiconducting SWCNTs under both tensile and torsional strains: (a) (8,0) and (b) (8,4) tube. Here, the applied tensile strains are fixed at 5%, and the torsional ones are taken to be 6.6° and −3.0°, respectively, for the (8,0) and (8,4) tubes.

present E_{33}, as shown in Fig. 4(b). In addition, it is worth noticing that for perfect (5,5) tube and the deformed (5,5) tube under pure tensile strain, its LO mode is *not* Raman active. However, the torsional strain destroys its LO mode symmetry, making now its LO mode to be Raman-active, but unfortunately its intensity is very smaller, which is caused by its very small electron-phonon matrix element M_{33}. While under both tensile and torsional strains, the Raman intensity of its LO mode is found to increase, compared with that under pure torsional strain. That is because the superposed tensile strain changes the vibration direction of its LO mode, increasing its electron-phonon matrix element M_{33}. So, it is obvious that under both tensile and torsional strains, the resonant Raman spectra of armchair (5,5) tube does not equal to a simple summation over those induced by the separate strains, which is different from the situation of zigzag tube. This fact reflects again the importance of the so-called interference effect and further shows the dependence of the interference effect on the tube's chirality and mode symmetry. Finally, it is found from Fig. 4(c) that (8,4) tube has the similar results to those of (10,0) tube, except that tensile strain decreases a little bit its TO mode intensity.

We have known from Fig. 4 that (1) the *G*-band LO mode intensity is increased (decreased) by tensile (torsional) strain. In contrast, the TO mode intensity is increased by torsional strain, but almost not influenced by tensile strain. (2) For the lower-energy RBM mode intensity, tensile strain has little effect on it, but torsional strain seems to increase it a little bit for (5,5) and (8,4) tubes.

Now, it is interesting to know if the above results on the first-order resonant Raman intensity of different deformed SWCNTs will change when the resonances happen at different electronic transition energies. In order to make it clear, we have calculated them when the resonance takes place at the lower electronic transition energies, which are given in Fig. 5 for different semiconducting (8,0) and (8,4) SWCNTs under both tensile and torsional strains, where the tensile strain is taken to be 5%, and the torsional angle is 6.6° for zigzag (8,0) tube and −3.0° for chiral (8,4) tube.

It is found from Fig. 5 that torsional strain own increases (but decreases) the TO (LO) mode intensity, which is the same as the situation shown in Fig. 4. Thus, the intensity changes of both the LO and TO modes, induced by pure torsional strain, are independent of the electronic transition energy and the tube's chirality. However, the tensile strain plays a different role. For example, for (8,0) tube [Fig. 5(a)], its LO mode intensity is increased by tensile strain at the resonance with the E_{21}, which is upshifted by pure tensile strain relative to its position at zero tensile strain. But for (8,4) tube [Fig. 5(b)], its LO mode intensity is decreased by tensile strain at the resonance with the E_{22}, which is downshifted by pure tensile strain relative to its position at zero tensile strain. So, comparing with Fig. 4, we have known that the LO mode intensity changes, induced by pure tensile strain, have a close relation with the tube's chirality and also the corresponding shift of the electronic transition energy.

Under both tensile and torsional strains, for the upshifted E_{21} of (8,0) tube, it is found from Fig. 5(a) that the intensity changes of the resonant Raman spectra can indeed be considered as the simple summation of those induced by the separate tensile and torsional strains. But it is different for the downshifted E_{22} of (8,4) tube, as shown in Fig. 5(b), from which we can see that the intensity at the $E_{22}+E_{LO}$ of the (8,4) tube under both tensile and torsional strains is not

decreased, compared with that under pure torsional strain. Because tensile strain own decreases the intensity at the $E_{22}+E_{LO}$, so the intensity changes of the resonant Raman spectra at the downshifted E_{22} of (8,4) tube, induced by both tensile and torsional strains, cannot be seen as the simple summation of those from the separate tensile and torsional strains.

In a word, it seems that torsional strain would increase (decrease) the resonant Raman intensity of the *G*-band TO (LO) mode of deformed SWCNTs. In contrast, tensile strain would have little effect on the resonant Raman intensities of their TO modes, but increase (decrease) them of their LO modes at resonance with their upshifted (downshifted) electronic transition energies. The RBM mode intensity changes are found to depend on the tube chirality and deformation types.

When both tensile and torsional strains are applied, the intensity changes in the resonant Raman spectra at the upshifted electronic transition energy due to tensile strain can be seen as the simple summation of those from the separate tensile and torsional strains, but it is not for the downshifted electronic transition energy, indicating also existence of the interference effects between both tensile and torsional strains on the intensity changes.

Finally, we would like to mention that our above calculated results on the intensity changes under combined tensile and torsional strains are partially supported by the experimental results,[8,24] e.g., the resonant Raman intensity variation depends on the different types of strains, tubes, and modes. That is probably because all these factors would induce significantly different responses of the tube's electronic structures and electron-phonon coupling matrix to the strains.

IV. CONCLUSIONS

In summary, using the nonorthogonal TB model, we have found that the frequency shifts of the Raman-active modes of deformed SWCNTs due to tensile and torsional strains depend much on the C-C bond length changes in the corresponding tubes. It is found that (1) the frequencies of low-energy Raman modes nearly do not change by two kinds of the strains. (2) In contrast, tensile strain downshifts the frequencies of high energy Raman modes. But, the corresponding changes due to torsional strain depend on the tube's chirality and the mode symmetry. (3) The resonant Raman intensity of deformed SWCNTs is found to depend on the strain type and mode symmetry, e.g., torsional strain increases (decreases) the resonant Raman intensity of the TO (LO) mode, and tensile strain has little effect on that of the TO mode, but increases (or decreases) that of the LO mode, depending on the selected electronic transition energy. (4) More interestingly, there exists an interference (or cooperative) effects between the tensile and torsional strains on the strain-induced frequency shifts and intensity changes, depending on the tube's chirality and mode symmetry, which need more future experimental and theoretical works for demonstration.

ACKNOWLEDGMENTS

*Corresponding author; jdong@nju.edu.cn

[1] S. Iijima, Nature (London) **354**, 56 (1994).

[2] M. S. Dresselhaus, G. Dresselhaus, and Ph. Avouris, *Carbon Nanotubes: Synthesis, Structure, Properties and Applications*, Springer Series in Topics in Applied Physics Vol. 80 (Springer Verlag, Berlin, 2001).

[3] M. S. Dresselhaus, G. Dresselhaus, R. Saito, and A. Jorio, Phys. Rep. **409**, 47 (2005).

[4] R. Saito, G. Dresselhaus, and M. S. Dresselhaus, *Physical Properties of Carbon Nanotubes* (Imperial College Press, London, 1998).

[5] A. M. Rao, E. Richter, S. Bandow, B. Chase, P. C. Eklund, K. A. Williams, S. Fang, K. R. Subbaswamy, M. Menon, A. Thess, R. E. Smalley, G. Dresselhaus, and M. S. Dresselhaus, Science **275**, 187 (1997).

[6] A. G. Souza Filho, S. G. Chou, Ge. G. Samsonidze, G. Dresselhaus, M. S. Dresselhaus, L. An, J. Liu, A. K. Swan, M. S. Ünlü, B. B. Goldberg, A. Jorio, A. Grüneis, and R. Saito, Phys. Rev. B **69**, 115428 (2004).

[7] J. Jiang, R. Saito, A. Grüneis, S. G. Chou, G. G. Samsonidze, A. Jorio, G. Dresselhaus, and M. S. Dresselhaus, Phys. Rev. B **71**, 205420 (2005).

[8] X. Duan, H. Son, B. Gao, J. Zhang, T. Wu, G. G. Samsonidze, M. S. Dresselhaus, Z. Liu, and J. Kong, Nano Lett. **7**, 2116 (2007).

[9] S. W. Lee, Goo-Hwan Jeong, and E. E. B. Campbell, Nano Lett. **7**, 2590 (2007).

[10] S. B. Cronin, A. K. Swan, M. S. Ünlü, B. B. Goldberg, M. S. Dresselhaus, and M. Tinkham, Phys. Rev. B **72**, 035425 (2005).

[11] B. Gao, X. Duan, J. Zhang, G. Wu, J. Dong, and Z. Liu, J. Phys. Chem. C **112**, 10789 (2008).

[12] S. B. Cronin, A. K. Swan, M. S. Ünlü, B. B. Goldberg, M. S. Dresselhaus, and M. Tinkham, Phys. Rev. Lett. **93**, 167401 (2004).

[13] A. Merlen, N. Bendiab, P. Toulemonde, A. Aouizerat, A. San Miguel, J. L. Sauvajol, G. Montagnac, H. Cardon, and P. Petit, Phys. Rev. B **72**, 035409 (2005).

[14] U. D. Venkateswaran, E. A. Brandsen, U. Schlecht, A. M. Rao, E. Richter, I. Loa, K. Syassen, and P. C. Eklund, Phys. Status Solidi B **223**, 225 (2001).

[15] R. Heyd, A. Charlier, and E. McRae, Phys. Rev. B **55**, 6820 (1997).

[16] D. W. Brenner, J. D. Schall, J. P. Mewkill, D. A. Shenderova, and S. B. Sinnott, J. Br. Interplanet. Soc. **51**, 137 (1998).

[17] C. L. Kane and E. J. Mele, Phys. Rev. Lett. **78**, 1932 (1997).

[18] L. Yang, M. P. Anantram, J. Han, and J. P. Lu, Phys. Rev. B **60**,

13874 (1999).

[19] L. Yang and J. Han, Phys. Rev. Lett. **85**, 154 (2000).

[20] T. W. Tombler, C. Zhou, L. Alexseyev, J. Kong, H. Dai, L. Liu, C. S. Jayanthi, M. Tang and Shi-Yu Wu, Nature (London) **405**, 769 (2000).

[21] E. D. Minot, Y. Yaish, V. Sazonova, Ji-Yong Park, M. Brink, and P. L. McEuen, Phys. Rev. Lett. **90**, 156401 (2003).

[22] J. Cao, Q. Wang, and H. J. Dai, Phys. Rev. Lett. **90**, 157601 (2003).

[23] R. J. Grow, Q. Wanf, J. Cao, D. Wang, and H. Dai, Appl. Phys. Lett. **86**, 093104 (2005).

[24] B. Gao, X. Duan, J. Zhang, T. Wu, H. Son, J. Kong, and Z. Liu, Nano Lett. **7**, 750 (2007).

[25] H. Maki, T. Sato, and K. Ishibashi, Nano Lett. **7**, 890 (2007).

[26] M. Huang, Y. Wu, B. Chandra, H. Yan, Y. Shan, T. F. Heinz, and J. Hone, Phys. Rev. Lett. **100**, 136803 (2008).

[27] G. Wu, J. Zhou, and J. Dong, Phys. Rev. B **72**, 115411 (2005).

[28] M. Machón, S. Reich, H. Telg, J. Maultzsch, P. Ordejón, and C. Thomsen, Phys. Rev. B **71**, 035416 (2005).

[29] M. Machón, S. Reich, and C. Thomsen, Phys. Rev. B **74**, 205423 (2006).

[30] J. Jiang, R. Saito, G. G. Samsonidze, S. G. Chou, A. Jorio, G. Dresselhaus, and M. S. Dresselhaus, Phys. Rev. B **72**, 235408 (2005).

[31] V. N. Popov, L. Henrard, and P. Lambin, Nano Lett. **4**, 1795 (2004).

[32] V. N. Popov and P. Lambin, Physica E (Amsterdam) **37**, 97 (2007).

[33] I. Milošević, B. Nikolić, and M. Damnjanović, Phys. Rev. B **69**, 113408 (2004).

[34] V. N. Popov and L. Henrard, Phys. Rev. B **70**, 115407 (2004).

[35] D. Porezag, Th. Frauenheim, Th. Köhler, G. Seifert, and R. Kaschner, Phys. Rev. B **51**, 12947 (1995).